Title

Resolving space and time variation of lake-atmosphere carbon dioxide fluxes using multiple methods

Authors

Angela K. Baldocchi[1], David E. Reed[1,2], Luke C. Loken[3], Emily H. Stanley[3], Hayley Huerd[4], Ankur R. Desai[1]

1 University of Wisconsin-Madison, Department of Atmospheric and Oceanic Sciences, Madison, Wisconsin
2 Michigan State University, Center for Global Change and Earth Observations, East Lansing, Michigan
3 University of Wisconsin-Madison, Center for Limnology, Madison, Wisconsin
4 University of California Merced, Merced, California

Corresponding Author

David E. Reed

Abstract

Lakes emit globally significant amounts of carbon dioxide (CO_2) to the atmosphere, but quantifying these rates for individual lakes is extremely challenging. The exchange of CO_2 across the air-water interface is driven by physical, chemical, and biological processes in both the lake and the atmosphere that vary at multiple spatial and temporal scales. None of the methods we use to estimate CO_2 flux fully capture this heterogeneous process. Here, we compared concurrent CO_2 flux estimates from a single lake based on commonly used methods. These include floating chambers (FC), eddy covariance (EC), and two concentration gradient based methods labelled fixed (F-pCO_2) and spatial (S-pCO_2). At the end of summer, cumulative carbon fluxes were similar between EC, F-pCO_2 and S-pCO_2 methods (-4, -4 and -9.5 gC), while methods diverged in directionality of fluxes during the fall turnover period (-50, 43 and 38 gC). Collectively these results highlight the discrepancies among methods and the need to acknowledge the uncertainty when using any of them to approximate this heterogeneous process.

Plain Language Summary

Lakes comprise a small percentage of the landscape, but they are active and complex areas of carbon cycling. Lakes receive mixed carbon inputs from upstream sources, process this carbon internally, store it in sediments and biomass, and export it downstream. In addition, some fraction of the carbon in lakes exchanges into and out of the atmosphere, linking lakes with the global atmosphere. The exchange of carbon dioxide across lake surfaces has globally significant implications but quantifying these rates has yet to be fully resolved. Here, we compared four methods of estimating diffusive carbon dioxide exchange between the atmosphere and the lake surface. Flux rates generally agreed during the summer, but estimates diverged in the fall, a critical time period with elevated carbon cycling rates. These discrepancies among methods may arise because of the high degree of spatial and temporal variability in gas exchange and our ability to portray these processes accurately. In the future, we need to improve our observational resolution to better estimate carbon gas exchange between lakes and the atmosphere.

Key Points

1) Lake-atmosphere CO_2 exchange estimate using four common methods
2) CO_2 concentration gradient flux estimates agreed in direction and magnitude with floating chambers but disagreed with eddy covariance.
3) Inconsistencies among methods highlight the spatial and temporal assumptions underlying methods and the need to acknowledge uncertainty

Author Contribution Statement

DER and ARD collected eddy covariance data, LCL and EHS spatial gradient data, EHS and ARD collect fixed spatial gradient data, while HH and AKB collected chamber data. AKB led analysis with assistance from DER and LCL. AKB and DER drafted the manuscript, all authors helped edit the manuscript.

Competing Financial Interests

The authors declare no competing financial interests.

1. Introduction

Lakes are a major component of the Earth's carbon cycle and an increasing focus has been placed on carbon dynamics within inland waters [*Biddanda*, 2017; *Tranvik et al.*, 2009; *Williamson et al.*, 2009]. A substantial fraction of the organic carbon that is delivered to or fixed within lakes is outgassed to the atmosphere as carbon dioxide (CO_2) [*Cole et al.*, 2007; *Cory et al.*, 2014]. While there is consensus that collectively lakes and other inland waters emit meaningful amounts of CO_2 to the atmosphere, it remains extremely difficult to calculate spatially and temporally resolved emission rates for individual lakes. This difficulty is because the exchange of CO_2 across the air-water interface is driven by multiple physical, chemical, and biological processes in both the lake and the atmosphere that vary at multiple spatial and temporal scales. The scientific community lacks methods to fully capture the spatial and temporal heterogeneity in gas exchange between lakes and the atmosphere. Thus, every estimate of global CO_2 emissions from lakes has uncertainty.

The reason that lake-atmosphere fluxes are difficult to quantify is because they vary in magnitude [*Raymond et al.*, 2013], in time [*Reed et al.*, 2018], and across space [*Natchimuthu et al.*, 2016]. In many temperate dimictic lakes, seasonal phenologies in ice-cover and stratification govern the direction and magnitude of CO_2 flux. Large off-gassing events occur during periods of vertical mixing such as ice-off and fall turnover [*Denfeld et al.*, 2016]. Lakes with higher productivity show pronounced temporal variation in CO_2 flux [*S C Maberly et al.*, 2013] , characterized by influx during the summer periods coinciding with higher rates of primary production [*Reed et al.*, 2018]. Thus, for even a single lake, flux estimation needs to be continuous and year-round in order to capture the temporal heterogeneity in gas exchange. Spatially, heterogeneity in metabolic processes, hydrology, and turbulence can have pronounced

impacts on CO_2 flux from the lake surface. Rivers flowing into lakes typically differ in a number of physical, chemical, and biological properties that can create contrasts in pCO_2 in habitats where they enter a lake [*Chmiel et al.*, 2019]. Further, spatial heterogeneity varies temporally [*L C Loken et al.*, 2019; *Natchimuthu et al.*, 2016] due to changes in river flow, lake mixing, and biological processes. Thus, to accurately measure CO_2 flux from a single lake we need to incorporate both spatial and temporal processes.

Any calculations of lake-atmosphere CO_2 flux are limited in either special or temporal extent. Perhaps the simplest and most cost-effective method for measuring gas efflux from lakes is using floating chambers (FC) [*Bastviken et al.*, 2015]. Chambers are placed atop the lake surface and the flux is derived from the gas accumulation rate within the chamber. However, flux chambers characterize only a small area of the lake for what is typically a short deployment, and can alter turbulence and thus gas exchange within the chamber environment [*Vachon et al.*, 2010]. Historically, FC's for CO_2 required manual gas sampling followed by laboratory determination of gas concentrations, while newer FCs integrate continuous CO_2 sensors and automatic purging mechanisms that allow for longer deployments [*Bastviken et al.*, 2015; *Jonsson et al.*, 2008; *Martinsen et al.*, 2018]. While a single measurement is small in its spatial scale, multiple chambers have been used to quantify the spatial variability of gas emissions within and among lake habitats [*Natchimuthu et al.*, 2016; *Tangen et al.*, 2016]. Similarly, measuring temporal variability of fluxes using FCs is common but in both cases, characterizing spatial and/or temporal variability with this approach is time intensive. New automated chambers show promise in increasing the duration of continuous observation [*Duc et al.*, 2012].

A common alternative to FCs is modeling exchange rates using the concentration gradient or boundary layer method (F-pCO_2) [*Cole and Caraco*, 1998] that is based on

differences in pCO_2 between the lake surface and the atmosphere and an estimate of water turbulence or gas transfer velocity (k). Spatial scales of pCO_2 measurements within the water column are on the order of cubic centimeters and typically fixed in space. Estimation of k is typically based on empirically derived models using wind-speed, lake size, and/or water density gradients [*Crusius and Wanninkhof*, 2003; *MacIntyre et al.*, 2010; *Read et al.*, 2012]. k can also change in response to environmental conditions [*Natchimuthu et al.*, 2016; *Vachon and Prairie*, 2013]; moreover, estimation of k can vary by multiple orders of magnitude simply due to model choice [*Dugan et al.*, 2016]. Recent pCO_2 studies have shown the scaling k from point measurements to the lake scale strongly underestimates emissions [*Mammarella et al.*, 2015; *Schubert et al.*, 2012]. New methods have been developed to quickly quantify spatial variation in pCO_2 and k [*Bastviken et al.*, 2015; *Crawford et al.*, 2015] and have revealed substantial spatial variations in pCO_2 and fluxes within individual lakes and reservoirs [*L C Loken et al.*, 2019; *Natchimuthu et al.*, 2016; *Paranaíba et al.*, 2018]. Boundary layer methods have provided the most frequent and comprehensive understanding of CO_2 exchange between lakes and the atmosphere, yet most assume spatial homogeneity and are reliant on physical lake models that have large uncertainty.

A third approach for quantifying lake CO_2 fluxes is eddy covariance (EC) [*Morin et al.*, 2018; *Reed et al.*, 2018]. In contrast to the water-based approaches, EC uses measurements of concentrations of gas in the atmosphere along with high-frequency measurements of wind speeds in 3 dimensions. While this top-down flux method seems like the silver bullet for quantifying CO_2 flux, EC has several assumptions built into estimation and is spatially limited. It relies on measurement during windy periods and includes uncertainty of footprint models that estimate the area over which fluxes are being measured (i.e., the footprint), with a single flux estimate

integrating over 100's of square meters. Turbulence and footprint issues can lead to upwards of 80% of EC data being excluded [*Reed et al.*, 2018]. EC estimates represent the average flux from a portion of the lake surface, which bias observations toward near-shore areas [*Morin et al.*, 2018] where most towers are located. Despite these limitations, EC offers a promising method for assessing carbon fluxes from lakes [*Vesala et al.*, 2012].

Because each technique for measuring carbon flux has its limitations, efforts have been made to compare these methods. However, these investigations have been limited to relatively short time periods [*Erkkila et al.*, 2018; *Podgrajsek et al.*, 2016; *Schubert et al.*, 2012]. These authors found discrepancies among methods for quantifying CO_2 flux in both space and time. While estimates of carbon fluxes are critical for global carbon cycling, how best to measure lake-atmosphere fluxes remains challenging and is an open question for the scientific community.

In order to compare methods of quantifying lake-atmosphere fluxes of CO_2, we leveraged multiple concurrent datasets from a single north temperate lake (Lake Mendota, Wisconsin, USA). This lake has been subject to prior CO_2 flux investigations [*L C Loken et al.*, 2019; *Reed et al.*, 2018]. Here, we combined flux records based on measurements of pCO_2 at a moored buoy, measurements distributed across the entire lake surface, EC from a tower located at the end of a narrow peninsula, and FC. The overarching question of this work is: Are lake-atmosphere CO_2 flux estimates consistent among pCO_2, FC, and EC methods? Due to multiple temporal and spatial scales which the independent observations are taken over, we seek to answer the question using 1) analysis of flux distribution over multiple seasons, 2) quantifying cumulative sums of carbon flux, 3) direction comparison of methods, and 4) spectral time-series analysis of fluxes.

2. Methods

2.1 Site Description

Lake Mendota is a well-studied lake located in Southern Wisconsin, USA (43.1° N, 89.4° W) and is part of the North Temperate Lakes Long-Term Ecological Research (NTL-LTER) program. It is dimictic and eutrophic, with a surface area of 39.9 km^2, a maximum depth of 25.3 m (mean 12.7 m). The majority of the lake's watershed is composed of agricultural and urban land uses, resulting in elevated nutrient concentrations and high productivity [*Carpenter et al.*, 2007]. Thermal stratification typically occurs between May and October and ice cover from late December through March. We defined seasons using water column temperature gradients with spring and fall as periods in which the water column was isothermal, while in summer the lake was thermally stratified.

2.2 Flux Estimates

2.2.1 Fixed point concentration gradient method (F-pCO_2)

Since 2006, NTL-LTER has managed a monitoring buoy on Lake Mendota that is moored above the lake's deepest point (43.0995°N, 89.4045°W). The buoy is equipped with meteorological and limnological sensors and is deployed seasonally (~April through October), capturing the majority of the ice-free season. In 2015, a Turner Designs C-sense pCO_2 sensor (Turner Designs, San Jose, USA; 3% accuracy) was added to the buoy and installed at 0.5 m depth. For this study, we used wind speed, surface water temperature, and surface pCO_2 [*Magnuson et al.*, 2019]. Wind speed was measured at a height of 2.7 m above the lake surface using an anemometer (R. M. Young Marine Wind Monitor). Water temperature and pCO_2 were measured at a depth of 0.5m using a RBR concerto thermistor string and a Turner C-Sense CO_2 sonde, respectively. Wind speed and water temperature were measured every 30 minutes, while

177 pCO_2 was measured every 15 minutes. $pCO2$ in air was measured from an in situ spectroscopy
178 gas analyzer (Picarro, inc. 4-Species Gas Analyzer) located at a nearby building,

179 Using data collected at the buoy, we calculated the diffusive efflux of CO_2 from the lake
180 surface to the atmosphere according to:

181 $$Flux = k_{gas}\ x\ kh\ x\ (pCO_{2water} - pCO_{2air}) \quad (1)$$

182 This fixed-point boundary layer method (F-pCO_2) is based on the partial pressure gradient
183 between the water (pCO_{2water}) and the atmosphere (pCO_{2air}). Multiplying this difference by the
184 Henry's law constant *(kh*) converts to molar units and by the gas transfer velocity (k_{gas}) to
185 generate diffusive flux estimates. We estimated k_{gas} using concurrent wind speed and water
186 temperature recorded at the buoy, applying the k_{600} model and Schmidt model coefficients
187 provided in *Raymond et al.* [2013]. The Henry's law constant (*kh*) was calculated using
188 atmospheric pressure and temperature-dependence models provided in *Plummer and Busenberg*
189 [1982] See *L C Loken et al.* [2019] for further description of the pCO_2 flux model. pCO_2 flux
190 estimates were computed at 30-minute intervals. To temporally match observations between
191 methods, a subset of F-pCO_2 was used from 8 a.m.-12:00 p.m., the time period that overlapped
192 with the majority (>90%) of the spatially-explicit pCO_2 sampling times (described below).
193

194 **2.2.2 Spatial concentration gradient method (S-pCO_2)**

195 In addition to the F-pCO_2-based flux estimation at the buoy, we also compared flux
196 estimates using pCO_2 measurements from the entire lake surface (S-pCO_2) from *L C Loken et al.*
197 [2019]. For the entire ice-free period of 2016, [*L C Loken et al.*, 2019] generated CO_2 efflux
198 estimates at 988 points distributed in a gridded pattern across the lake surface. Efflux
199 measurements were based on measurements of pCO_2 that were distributed across the entire lake

surface. Similar to the F-pCO_2 method, efflux was calculated using the difference in pCO_2 between the water and the air. *L C Loken et al.* [2019] used a spatially explicit *k* model [*Vachon and Prairie*, 2013], which takes into account wind speed and direction and allows *k* to vary across the lake surface. pCO_2 measurements were collected over a ~3-hour window in the morning during each survey, and efflux was estimated at daily time scales. Two subsets of S-pCO_2 data was used to quantify spatial variability, 10 stratified random points from the entire lake and S-pCO_2 measurement locations from within the EC footprint.

2.2.3 Flux Chamber Diffusion Method (FC)

We conducted four FC campaigns between July 6, 2017 and April 24, 2018. CO_2 sensors (Sensair K30) were installed inside floating chambers with a diameter of 0.3 m and a height of 0.12 m. Flux rates were calculated using the chamber dimensions (surface area and volume) and continuous pCO_2 measurements within the enclosed headspace. Each 24-hr sampling campaign consisted of 7 sampling trips spaced every 4 hours with the goal of measuring flux rates over a complete diel cycle. For each measurement, we placed two chambers on the lake surface in the middle of the lake (same location as the buoy) and let them drift for 5 minutes. We repeated the FC procedure 3 times per chamber and calculated the average of the 6 flux measurements. CO_2 flux was calculated as:

$$Flux = \frac{\Delta pCO_2}{\Delta t} \times \frac{V}{SA} \quad (2)$$

where V is the chamber volume (0.03114 m^3), SA is the chamber bottom area (0.071 m^2), and *t* is time (s). Prior to the first campaign, we calibrated all sensors using N_2 gas and the "zero calibration" method per *Bastviken et al.* [2015]. For all subsequent campaigns we re-confirmed the zero CO_2 readings using N_2 gas.

2.2.4 Eddy Covariance Tower

Eddy covariance flux observations (Ameriflux site: US-PnP, doi: 10.17190/AMF/1433376) were collected from a tower at the end of a ~50 m wide peninsula on the shore of Lake Mendota (Figure 1) starting on June 20, 2016. These flux observations were made with a sonic anemometer (CSAT3, Campbell Scientific, Logan UT, USA) and open-path infrared gas analyzer for CO_2 and water vapor gas concentration (LI-7500A, Li-Cor, Lincoln, NE, USA) at a height of 12.4 m above the lake on a 0.95 m boom, along with measurements of air temperature and humidity (Vaisala, Inc. HMP45C). Measurements of incoming solar radiation and atmospheric pressure were collected from a nearby meteorological tower located on the roof of the Atmospheric, Oceanic, and Space Sciences building.

Eddy fluxes were calculated based on the covariance of vertical wind velocity and scalar concentrations following the approach of *Mauder and Foken* [2015], with quality control flags for stationarity, integral turbulence, and propagates estimates of random error. Using an eddy flux surface flux footprint model [*Kljun et al.*, 2015], we identified and removed non-lake data at 30-minute time-scales, primarily when winds were from the forested portion of the peninsula. After footprint screening and quality control, 26% of data were remaining.

2.3 Comparison of methods

Flux estimates varied in temporal and spatial coverage (Table 1). EC-based fluxes were collected continuously since 2016. Buoy-based F-*p*CO2 estimates are also continuous since this time, with the exception of winter months. We only have S-*p*CO2 rates for the ice-free period of 2016, which were collected ~weekly and daily rates were modelled by interpolating pCO_2

through time (see *L C Loken et al.* [2019] for details). Thus, these three data sources (S-pCO_2, F-pCO_2, and EC) overlapped throughout the ice-free period in 2016. We collected FC flux rates seasonally starting in summer 2017 (July 28-29, 2017, Oct 28-29, 2017, and April 23-24, 2018). Thus, there are three 24-hr intervals where FC, EC, and F-pCO_2 estimates overlapped in time. In addition to temporal overlap, we must also consider spatial coverage as sampling sites varied among methods. Both the FC- and F-pCO_2-based rates were determined at the center of the lake. The EC rates reflect the area surrounding the tower along the lake's southern shoreline, and S-pCO_2 covered the entire lake surface (Figure 1).

Because of varying temporal resolution among datasets, we converted all datasets to daily averages, representing the coarsest temporal scale. Using the S-pCO_2 flux estimates, we generated two additional spatial datasets. First we randomly selected 10 stratified points from the entire lake to visualize spatial variability across the lake. Second, we subset the S-pCO_2 dataset by only including flux estimates from within the EC footprint for a comparison between these two methods that was not confounded by differences in sampling areas. Cumulative fluxes from 2016 were calculated from F-pCO_2, S-pCO_2, and EC observations.

In addition to comparing similarity in seasonal pattern and magnitude, we also wanted to determine if the different methods exhibited similar temporal variance. To do so, we calculated Fourier power spectra of each daily time series. Data analysis was done in Matlab R2019a and IDL 8.6.0.

3. Results

3.1 Patterns among methods

Footprint modeling revealed that the EC footprint originated primarily from open water, with very little apparent input from the terrestrial peninsula (Figure 2a), with the distance of maximum contribution of fluxes on average being 40 m while the distance containing 80% of flux contribution was 410 m. Friction velocity (u*) values were high due to winds crossing the peninsula, showing increased turbulence due to the tree canopy (Figure 2b). While winds originated from all directions, wind speeds were lower over the peninsula as well (Figure 2c). These factors combined to limit the footprint along the narrow range of wind directions over the peninsula.

In all years, F-pCO_2 flux estimates followed a similar pattern of near-zero or slightly negative fluxes denoting CO_2 movement from the atmosphere to the lake during spring and summer months before becoming strongly positive (net CO_2 efflux from the lake to the atmosphere) in the fall (Figures 3, 4). Daily-averaged fluxes varied from -1.2 to 4.1 μm m^{-2} s^{-1} across all dates with a CV of 8.42. This same pattern was also demonstrated by the S-pCO_2 method (Figures 3, 4), and flux estimates were similar in magnitude and direction as the F-pCO_2 results in 2016 (-0.39 to 1.6 μm m^{-2} s^{-1}, CV of 6.34). The limited set of FC deployments also followed the same general pattern of CO_2 influx to the lake in spring, a weaker influx during summer, and efflux in the fall (Figure 3b-d). However, the range of FC flux values were narrower than for the two pCO_2-based methods (-1.6 to 2.1 μm m^{-2} s^{-1}, CV of 8.72).

Fluxes derived from the EC method were characterized by higher variation, often shifting from negative to positive fluxes within a period of 1-3 days. Daily-averaged fluxes varied from -22.5 to 18 μm m^{-2} s^{-1}, and the coefficient of variation was 3.13. There were no clear seasonal patterns in terms of magnitude, direction, or variance, although large CO_2 uptakes were recorded

prior to ice-on in both 2016 and 2017 and negative- and smaller positive fluxes were more common during ice-covered winter days.

3.2 Comparisons among methods

Differences among methods were clearly illustrated when flux data were expressed as cumulative flux (Figure 5). All methods indicated the lake was a slight CO_2 sink over the summer; however, estimates diverged substantially during fall. Both the S-pCO_2 and F-pCO_2 methods consistently indicated CO_2 flux into the lake all summer and substantial CO_2 flux out of the lake during fall. At the end of the year, the cumulative flux based on F-pCO_2 was 15% higher (43.4 vs 37.7 gC m^{-2}) than flux based on S-pCO_2, but both followed similar temporal trends. In contrast, the EC method suggested the lake fluctuated between CO_2 source and sink behavior with a high degree of variability on the weekly time-scale. At the end of summer (day ~268), the EC-based cumulative flux was comparable to the boundary layer-based rates. However, during fall, once mixing begins, the EC cumulative flux became progressively more negative, suggesting the lake became a more substantial CO_2 sink.

CO_2 fluxes based on FC (flux chamber) agreed in magnitude and direction with the F-pCO_2 during spring, summer, and fall (Figure 3b-d). Comparing FC with EC, the two methods disagreed in flux magnitude during summer and direction during fall.

The discrepancy between methods could be caused by the temporal or spatial resolution of observations. The day-time EC data more closely aligned with the F-pCO_2 and S-pCO_2 results during the summer. These methods agreed that the daytime flux of CO_2 during the summer was consistently into the lake. During the fall, the daytime EC fluxes remained negative, suggesting a consistent flux of CO_2 into the lake. Spatially, the S-pCO_2 results within the EC footprint were

consistent with the majority of the S-pCO_2 data. This suggests the lake was relatively homogeneous in regard to flux rates, with subset S-pCO_2 locations showing ~20% variability in accumulated fluxes at the end of the year. Temporal subsets of EC data show differences during the summer with the full-day EC data, but ultimately small differences in accumulated fluxes at the end of the year. Average EC error was 38.9%, with larger accumulated errors during the fall.

Directly comparing estimates using linear regression models further demonstrate the dissimilarity among methods. The two concentration gradient methods, F-pCO_2 and S-pCO_2, agreed in magnitude and direction ($R^2 = 0.55$, p value < 0.001; Figure 6a). When flux estimates were categorized by season, data from the summer were tightly clustered, while data from the fall were more scattered. Comparing EC to S-pCO_2 (Figure 6b), there was poor agreement ($R^2 = 0.07$; $p = 0.03$), and the regression model had a negative slope. Thus, daily flux rates using EC disagreed in direction with the concentration-based methods.

Fourier power spectral decomposition (Figure 7) of daily flux from EC, F-pCO_2 and S-pCO_2 data all had similar patterns over the quantifiable frequencies, with highest spectral power is seen in EC time-series, and S-pCO_2, and finally F-pCO_2. Seasonal and synoptic (3-10 day) variability dominate all three, though the EC tower also shows a sub-monthly (~20 day) mode of variability not seen in the other two.

4. Discussion

Few studies have used multiple measurements of long-term lake-atmosphere fluxes to address systemic biases in methods. Using concurrent long-term records from a single lake, we showed divergent behavior among flux estimates, particularly during the fall turnover period. EC-based calculations had large and opposing sign CO_2 flux estimates compared to FC and

concentration gradient-based methods (F-pCO_2 and S-pCO_2). FC-based methods agreed in direction and magnitude as pCO_2-based methods, however we lack sufficient FC coverage to interrogate the validity of this agreement. Together, these results suggest that at least for this lake and these estimates, EC and concentration gradient methods for estimating CO_2 flux differ dramatically.

The spatial and buoy-based concentration gradient estimates closely agreed. Both estimates followed similar seasonal patterns, indicating that the lake was taking in CO_2 from the atmosphere during the summer, and emitted a substantial amount during the fall. The buoy-based data showed this seasonal phenology in three consecutive years [*Reed et al.*, 2018], aligning with other studies of productive lakes [*S Maberly*, 1996] and the perception that productive lakes behave as CO_2 sinks during the summer [*Balmer and Downing*, 2011]. The agreement between the spatial and buoy-based concentration data suggests low spatial heterogeneity in CO_2 fluxes across the surface of Lake Mendota. On average most of the lake surface was within a within a 0.2 μmol m^{-2} s^{-1} range in CO_2 flux [*L C Loken et al.*, 2019]. Thus, spatial variability is small compared to the seasonal variability from all our CO_2 flux methods (Figures 3 and 5). However, spatial heterogeneity increased during fall turnover, making the buoy location less representative of the whole lake during this period [*L C Loken et al.*, 2019]. During periods of chaotic water mixing, the representativeness of a single location decreases [*Erkkila et al.*, 2018]. Thus, we suspect the discrepancies among methodologies during the summer season are not due to spatial heterogeneity in gas exchange across the lake surface.

With a limited number of FC observations, FC data approximately matched F-pCO_2 and S-pCO_2 during the spring and summer. Comparing FC and F-pCO_2 methods, *López Bellido et al.* [2009] found that FC were systematically higher than F-pCO_2, due to site-specific and time-

specific gas transfer velocities. They used daily concentration measurements and hence were not able to access daily patterns. *Podgrajsek et al.* [2014] found that FC and EC fluxes generally agreed, except when pCO_2 varied within the EC footprint. This is expanded on to show higher eddy covariance CO_2 fluxes at night relative to F-pCO_2 and also that F-pCO_2 methods need to account for convection within the water column [*Podgrajsek et al.*, 2016]. *Erkkila et al.* [2018] found F-pCO_2-based estimates were lower than EC while those based on FC were higher than EC estimates. Together, there does not appear to be an emerging trend among results, other than EC fluxes can be typically higher at night.

k may be responsible for the discrepancy among flux estimates. The *k* model underlying our concentration gradient based methods may have not adequately portrayed turbulence at the lake surface. Convective mixing within the water column introduce error into F-pCO_2 methods [*Podgrajsek et al.*, 2016]. These models base *k* on wind speed, but the effects of individual wind events on lakes are highly variable. For example, two days with similar wind speed and direction likely do not have the identical patterns of surface turbulence, compounded with spatial variability of *k* across fine scales [*L C Loken et al.*, 2019]. Ultimately, concentration gradient-based estimates rely on measurements that have a spatial scale on the order of one liter, and while *k* parameter incorporates wind speed and convection at a broader scale, our *k* model does not account for processes at the finer scales. While only using short periods (1-3 days), *Eugster et al.* [2003] used eddy covariance and chambers from Alaska and Switzerland to show the importance of convective mixing due to lake-atmosphere fluxes, with significant differences between methods during periods of stratification and with deep, penetrative convection.

Another possible explanation is potential biases in EC measurements during periods of low turbulence, complex turbulence, or advection. *Morin et al.* [2018] noted in a model study the

role of tower height and lake-land circulations in driving eddy transport that would be bias traditional flux calculation based on half-hourly Reynold's decomposition. As the surface cools, enhanced low-level atmospheric stability may suppress turbulence, leading to larger than typical storage or advective contribution to surface fluxes [*Lee et al.*, 2004]. As noted by *Xu et al.* [2019], below-sensor storage flux calculation can be critical to correcting tower-measured flux to represent surface flux, especially periods around sunrise and sunset. However, while we lack storage flux observations at this site or models of local circulation and turbulence on the peninsula, and there is no evidence in the data of a preferential circulation during fall or other periods of stable conditions. Further work on data quality filtering of EC over lakes is necessary to build confidence in its use over lakes.

EC may have other benefits, even when subject to potential systematic bias. Here, when examining the spectral density of the multiple observations, the EC observations show a 20-30 day frequency not observed by the other methods, including the similarly high frequency buoy measurements. *Eugster et al.* [2003] also concludes that EC methods should be used in order to collect process-scale data from the full season. Similarly, *Podgrajsek et al.* [2016] suggests the high temporal resolution of EC is crucial to resolve diel changes in flux, combined with measurements within the water column with high (30 minute) frequency. *Reed et al.* [2018] used a different EC observation dataset on Lake Mendota, not used here due to a large amount of gaps from that tower's location during the study period, but showed high degrees of coherence between CO_2 flux and air temperature at a similar sub-monthly (20-30 day) timescale. An emerging trend in aquatic flux literature is this monthly timescale of variation where *Liu et al.* [2011]; *Liu et al.* [2016] connect synoptic weather patterns to mixing, and *Shao et al.* [2015] and

Ouyang et al. [2017] show monthly correlation between CO_2 flux and chlorophyll and algal blooms.

There are ways to capture this 20-30 day timescale without high temporal coverage. Previously *Natchimuthu et al.* [2016] used a long-term FC dataset and then sub-sampling the observations following the methods of *Wik et al.* [2016]. They concluded that only ≥8 measurement days, distributed over multiple seasons, and high enough spatial coverage (≥8 locations during summer, ≤5 during spring and fall) are key for representative (± 20%) flux estimates at the annual timescale. However, they note that the flux estimates would be biased if observations excluded episodic events such as lake circulation patterns, diel or seasonal variation, or high flux areas from a lake. Given the mismatch between what the EC literature is concluding about needing high temporal resolution observations and the FC literature about only needing ≥8 days for CO_2 [*Natchimuthu et al.*, 2016], with a lower average flux [*Wik et al.*, 2016], we argue that while it is possible to estimate annual fluxes from a small number of sample days, functionally we think it would be difficult to observe only 8 days of FC fluxes and have a high degree of confidence that we have captured the temporal processes needed. Ultimately, we do judge the flux signal found at the 20-30 day frequency as important and the best way to capture appears to be EC methods.

5. Conclusions

While major advances have been made, quantifying lake-atmosphere fluxes from individual lakes over multiple spatial and temporal scales, remains a challenge. We are becoming more aware of the importance of lakes in global and local carbon cycles. Accurately accounting

for temporally and spatially heterogeneity in the flux of carbon across lake surfaces is vital for incorporation and constraining process-based predictions within lake models.

Overall, there is a need for increased spatiotemporal resolution in studies of CO_2 exchange between lakes and the atmosphere. Long term temporal data collection is essential to capture, diel, 20-30 day, and seasonal patterns. Spatially, there is still an open question as to which method is capturing flux magnitude correctly, as each method integrates different processes into the observation. This is done most explicitly when choosing between multiple k models but is also implicated when screening EC data. There is no emerging trend in magnitude or direction between methods and additional work is needed to bridge spatiotemporal scales.

Acknowledgements

This study was supported by the National Science Foundation (NSF) Atmospheric and Geospace Sciences Postdoctoral Fellowship Program (#GEO-1430396) and the NSF Long-Term Ecological Research (LTER) program award to North Temperate Lakes (NTL) (#DEB-1440297). We would like to thank Jonathan Thom for field work help, Yost R. for keeping momentum going on the project and John Maginnis for his perseverance and assistance on the FC 2017-18 campaigns.

Data for eddy covariance (US-PnP) can be found at Ameriflux: http://dx.doi.org/10.17190/AMF/1433376. CO_2 concentrations used in the spatial (dataset 337, doi: doi:10.6073/pasta/fe9c5437f67254f521bf5f7e0308bf93) and temporal concentration gradient (dataset ID 129, doi:10.6073/pasta/9bced2f6ff81aa30f0f573766c0a410b) can be found at the NTL-LTER database at https://lter.limnology.wisc.edu/data and are indexed in the Environmental Data Initiative. Floating chamber data have been deposited into the Environmental Data Initiative database at https://doi.org/10.6073/pasta/f6a915989753aba6f18b6b095e7a52d0.

References

Balmer, M. B., and J. A. Downing (2011), Carbon dioxide concentrations in eutrophic lakes: undersaturation implies atmospheric uptake, Inland Waters, 1(2), 125-132.

Bastviken, D., I. Sundgren, S. Natchimuthu, H. Reyier, and M. Gålfalk (2015), Cost-efficient approaches to measure carbon dioxide (CO2) fluxes and concentrations in terrestrial and aquatic environments using mini loggers, Biogeosciences, 12(12), 3849-3859.

Biddanda, B. (2017), Global significance of the changing freshwater carbon cycle, Eos.

Carpenter, S. R., B. J. Benson, R. Biggs, J. W. Chipman, J. A. Foley, S. A. Golding, R. B. Hammer, P. C. Hanson, P. T. Johnson, and A. M. Kamarainen (2007), Understanding regional change: a comparison of two lake districts, Bioscience, 57(4), 323-335.

Chmiel, H. E., H. Hofmann, S. Sobek, T. Efremova, and N. Pasche (2019), Where does the river end? Drivers of spatiotemporal variability in CO
2
concentration and flux in the inflow area of a large boreal lake, Limnology and Oceanography, n/a(n/a), doi: 10.1002/lno.11378.

Cole, J. J., and N. F. Caraco (1998), Atmospheric exchange of carbon dioxide in a low-wind oligotrophic lake measured by the addition of SF6, Limnology and Oceanography, 43(4), 647-656.

Cole, J. J., et al. (2007), Plumbing the global carbon cycle: Integrating inland waters into the terrestrial carbon budget, Ecosystems, 10(1), 171-184, doi: 10.1007/s10021-006-9013-8.

Cory, R. M., C. P. Ward, B. C. Crump, and G. W. Kling (2014), Sunlight controls water column processing of carbon in arctic fresh waters, Science, 345(6199), 925-928.

Crawford, J. T., L. C. Loken, N. J. Casson, C. Smith, A. G. Stone, and L. A. Winslow (2015), High-Speed Limnology: Using Advanced Sensors to Investigate Spatial Variability in Biogeochemistry and Hydrology, Environmental Science & Technology, 49(1), 442-450, doi: 10.1021/es504773x.

Crusius, J., and R. Wanninkhof (2003), Gas transfer velocities measured at low wind speed over a lake, Limnology and Oceanography, 48(3), 1010-1017.

Denfeld, B. A., M. Ricão Canelhas, G. A. Weyhenmeyer, S. Bertilsson, A. Eiler, and D. Bastviken (2016), Constraints on methane oxidation in ice-covered boreal lakes, Journal of Geophysical Research: Biogeosciences, 121(7), 1924-1933, doi: 10.1002/2016jg003382.

Desai, A. (2018), AmeriFlux US-Pnp Lake Mendota, Picnic Point Site, edited, ; AmeriFlux; University of Wisconsin Madison.

Desai, A. R. (2019), GLEON DC-FLUX Lake Mendota floating chamber carbon dioxide flux, 2017-2018, Environmental Data Initiative, doi: doi:10.6073/pasta/1178a60f9e3997e3c3ad25ab6d6250fc.

Duc, N. T., S. Silverstein, L. Lundmark, H. Reyier, P. Crill, and D. Bastviken (2012), Automated flux chamber for investigating gas flux at water–air interfaces, Environmental science & technology, 47(2), 968-975.

Dugan, H. A., R. I. Woolway, A. B. Santoso, J. R. Corman, A. Jaimes, E. R. Nodine, V. P. Patil, J. A. Zwart, J. A. Brentrup, and A. L. Hetherington (2016), Consequences of gas flux model choice on the interpretation of metabolic balance across 15 lakes, Inland Waters, 6(4), 581-592.

Erkkila, K.-M., A. Ojala, D. Bastviken, T. Biermann, J. J. Heiskanen, A. Lindroth, O. Peltola, M. Rantakari, T. Vesala, and I. Mammarella (2018), Methane and carbon dioxide fluxes over a lake: comparison between eddy covariance, floating chambers and boundary layer method, Biogeosciences, 15(2), 429-445.

Eugster, W., G. Kling, T. Jonas, J. P. McFadden, A. Wüest, S. MacIntyre, and F. S. Chapin III (2003), CO2 exchange between air and water in an Arctic Alaskan and midlatitude Swiss lake: Importance of convective mixing, Journal of Geophysical Research: Atmospheres, 108(D12).

Jonsson, A., J. Åberg, A. Lindroth, and M. Jansson (2008), Gas transfer rate and CO2 flux between an unproductive lake and the atmosphere in northern Sweden, Journal of Geophysical Research: Biogeosciences, 113(G4), doi: 10.1029/2008jg000688.

Kljun, N., P. Calanca, M. W. Rotach, and H. P. Schmid (2015), A simple two-dimensional parameterisation for Flux Footprint Prediction (FFP), Geosci. Model Dev., 8(11), 3695-3713, doi: 10.5194/gmd-8-3695-2015.

Lee, X., W. Massman, and B. Law (2004), Handbook of Micrometeorology: A Guide for Surface Flux Measurement and Analysis, Kluwer, Dordrecht, The Netherlands.

Liu, H., P. D. Blanken, T. Weidinger, A. Nordbo, and T. Vesala (2011), Variability in cold front activities modulating cool-season evaporation from a southern inland water in the USA, Environmental research letters, 6(2), 024022.

Liu, H., Q. Zhang, G. G. Katul, J. J. Cole, F. S. Chapin III, and S. MacIntyre (2016), Large CO2 effluxes at night and during synoptic weather events significantly contribute to CO2 emissions from a reservoir, Environmental Research Letters, 11(6), 064001.
Loken, L., E. Stanley, P. Schramm, and M. Gahler (2019), Spatial surface water chemistry of Lake Mendota with FLAMe: 2014-2016.
Loken, L. C., J. T. Crawford, P. J. Schramm, P. Stadler, A. R. Desai, and E. H. Stanley (2019), Large Spatial and Temporal Variability of Carbon Dioxide and Methane in a Eutrophic Lake, J Geophys Res-Biogeo, 124(7), 2248-2266, doi: 10.1029/2019jg005186.
López Bellido, J., T. Tulonen, P. Kankaala, and A. Ojala (2009), CO2 and CH4 fluxes during spring and autumn mixing periods in a boreal lake (Pääjärvi, southern Finland), Journal of Geophysical Research: Biogeosciences, 114(G4), doi: 10.1029/2009jg000923.
Maberly, S. (1996), Diel, episodic and seasonal changes in pH and concentrations of inorganic carbon in a productive lake, Freshwater Biology, 35(3), 579-598.
Maberly, S. C., P. A. Barker, A. W. Stott, and M. M. De Ville (2013), Catchment productivity controls CO2 emissions from lakes, Nature Climate Change, 3(4), 391-394, doi: 10.1038/Nclimate1748.
MacIntyre, S., A. Jonsson, M. Jansson, J. Aberg, D. E. Turney, and S. D. Miller (2010), Buoyancy flux, turbulence, and the gas transfer coefficient in a stratified lake, Geophysical Research Letters, 37(24).
Magnuson, J., S. Carpenter, and E. Stanley (2019), North Temperate Lakes LTER: High Frequency Water Temperature Data-Lake Mendota Buoy 2006-current.
Mammarella, I., A. Nordbo, Ü. Rannik, S. Haapanala, J. Levula, H. Laakso, A. Ojala, O. Peltola, J. Heiskanen, and J. Pumpanen (2015), Carbon dioxide and energy fluxes over a small boreal lake in Southern Finland, Journal of Geophysical Research: Biogeosciences, 120(7), 1296-1314.
Martinsen, K. T., T. Kragh, and K. Sand-Jensen (2018), Technical note: A simple and cost-efficient automated floating chamber for continuous measurements of carbon dioxide gas flux on lakes, Biogeosciences, 15(18), 5565-5573, doi: 10.5194/bg-15-5565-2018.
Mauder, M., and T. Foken (2015), Documentation and Instruction Manual of the Eddy-Covariance Software Package TK3 (update), Univ., Abt. Mikrometeorologie.
Morin, T., A. Rey-Sánchez, C. Vogel, A. Matheny, W. Kenny, and G. Bohrer (2018), Carbon dioxide emissions from an oligotrophic temperate lake: An eddy covariance approach, Ecological Engineering, 114, 25-33.
Natchimuthu, S., I. Sundgren, M. Gålfalk, L. Klemedtsson, P. Crill, Å. Danielsson, and D. Bastviken (2016), Spatio-temporal variability of lake CH4 fluxes and its influence on annual whole lake emission estimates, Limnology and Oceanography, 61(S1), S13-S26.
Ouyang, Z., C. Shao, H. Chu, R. Becker, T. Bridgeman, C. Stepien, R. John, and J. Chen (2017), The effect of algal blooms on carbon emissions in western Lake Erie: An integration of remote sensing and eddy covariance measurements, Remote Sensing, 9(1), 44.
Paranaíba, J. R., N. Barros, R. Mendonça, A. Linkhorst, A. Isidorova, F. Roland, R. M. Almeida, and S. Sobek (2018), Spatially Resolved Measurements of CO2 and CH4 Concentration and Gas-Exchange Velocity Highly Influence Carbon-Emission Estimates of Reservoirs, Environmental Science & Technology, 52(2), 607-615, doi: 10.1021/acs.est.7b05138.
Plummer, L. N., and E. Busenberg (1982), The solubilities of calcite, aragonite and vaterite in CO2-H2O solutions between 0 and 90 C, and an evaluation of the aqueous model for the system CaCO3-CO2-H2O, Geochimica et cosmochimica acta, 46(6), 1011-1040.
Podgrajsek, E., E. Sahlée, and A. Rutgersson (2014), Diurnal cycle of lake methane flux, Journal of Geophysical Research: Biogeosciences, 119(3), 236-248.
Podgrajsek, E., E. Sahlée, D. Bastviken, S. Natchimuthu, N. Kljun, H. Chmiel, L. Klemedtsson, and A. Rutgersson (2016), Methane fluxes from a small boreal lake measured with the eddy covariance method, Limnology and Oceanography, 61(S1), S41-S50.
Raymond, P. A., J. Hartmann, R. Lauerwald, S. Sobek, C. McDonald, M. Hoover, D. Butman, R. Striegl, E. Mayorga, and C. Humborg (2013), Global carbon dioxide emissions from inland waters, Nature, 503(7476), 355.
Read, J. S., et al. (2012), Lake-size dependency of wind shear and convection as controls on gas exchange, Geophysical Research Letters, 39(9), L09405, doi: Artn L09405 10.1029/2012gl051886.
Reed, D. E., H. A. Dugan, A. L. Flannery, and A. R. Desai (2018), Carbon sink and source dynamics of a eutrophic deep lake using multiple flux observations over multiple years, Limnology and Oceanography Letters, 3(3), 285-292, doi: 10.1002/lol2.10075.

564 Schubert, C. J., T. Diem, and W. Eugster (2012), Methane emissions from a small wind shielded lake determined by
565 eddy covariance, flux chambers, anchored funnels, and boundary model calculations: A comparison, Environmental
566 science & technology, 46(8), 4515-4522.
567 Shao, C., J. Chen, C. A. Stepien, H. Chu, Z. Ouyang, T. B. Bridgeman, K. P. Czajkowski, R. H. Becker, and R. John
568 (2015), Diurnal to annual changes in latent, sensible heat, and CO2 fluxes over a Laurentian Great Lake: A case
569 study in Western Lake Erie, Journal of Geophysical Research: Biogeosciences, 120(8), 1587-1604.
570 Tangen, B. A., R. G. Finocchiaro, R. A. Gleason, and C. F. Dahl (2016), Greenhouse Gas Fluxes of a Shallow Lake
571 in South-Central North Dakota, USA, Wetlands, 36(4), 779-787, doi: 10.1007/s13157-016-0782-3.
572 Tranvik, L. J., et al. (2009), Lakes and reservoirs as regulators of carbon cycling and climate, Limnology and
573 Oceanography, 54(6), 2298-2314, doi: DOI 10.4319/lo.2009.54.6_part_2.2298.
574 Vachon, D., and Y. T. Prairie (2013), The ecosystem size and shape dependence of gas transfer velocity versus wind
575 speed relationships in lakes, Canadian Journal of Fisheries and Aquatic Sciences, 70(12), 1757-1764, doi:
576 10.1139/cjfas-2013-0241.
577 Vachon, D., Y. T. Prairie, and J. J. Cole (2010), The relationship between near-surface turbulence and gas transfer
578 velocity in freshwater systems and its implications for floating chamber measurements of gas exchange, Limnology
579 and Oceanography, 55(4), 1723-1732, doi: 10.4319/lo.2010.55.4.1723.
580 Vesala, T., W. Eugster, and A. Ojala (2012), Eddy covariance measurements over lakes, in Eddy covariance, edited,
581 pp. 365-376, Springer.
582 Wik, M., B. F. Thornton, D. Bastviken, J. Uhlbäck, and P. M. Crill (2016), Biased sampling of methane release from
583 northern lakes: A problem for extrapolation, Geophysical research letters, 43(3), 1256-1262.
584 Williamson, C. E., J. E. Saros, W. F. Vincent, and J. P. Smol (2009), Lakes and reservoirs as sentinels, integrators,
585 and regulators of climate change, Limnology and Oceanography, 54(6part2), 2273-2282.
586 Xu, K., N. Pingintha-Durden, H. Luo, D. Durden, C. Sturtevant, A. R. Desai, C. Florian, and S. Metzger (2019), The
587 eddy-covariance storage term in air: Consistent community resources improve flux measurement reliability,
588 Agricultural and Forest Meteorology, 279, 107734, doi: https://doi.org/10.1016/j.agrformet.2019.107734.
589

590 **Tables**

591 Table 1. Temporal duration, water/gas sampling frequency, and spatial extent and resolution for the four methods used to estimate
592 CO_2 fluxes in Lake Mendota between 2016 and 2018, along with data availability information.

Method	Measurement period	Sampling frequency	Spatial extent	Spatial resolution	Citation
Fixed point concentration gradient (F-pCO_2)	Open Water Seasons (approx. April-Oct) 2016	15 min	Single point	10 cm^3	*Magnuson et al.* [2019]
Spatial concentration gradient (S-pCO_2)	Mar-Dec 2016	14 d	whole lake	200 m^2	*L Loken et al.* [2019]
Flux chamber diffusion (FC)	4 measurement campaigns, Jul 2017 – Apr 2018	5 min sampling, every 4 hours for 24 hours	Single point	0.28 m^2	*A R Desai* [2019]
Eddy covariance (EC)	June 2016-August 2018	30 min	1 km^2	1 km^2	*A Desai* [2018]

Figures

Figure 1

Panel (a) Lake Mendota. Buoy (yellow) is deployed in the deepest part of the lake and is the location for the F-pCO_2 and FC flux estimates. The red circles are a stratified selection of data points from the S-pCO_2 method used in Figure 5. Grid section (orange with a center circle) of EC tower location and 1 km^2 footprint. Panel (b) 2016 average daily air (blue) and surface water (black) temperatures. Spatial gradient concentration measurements were taken on the 2016 days of year indicated by the (25 orange) vertical lines. Dashed line (gray) at 20°C used to symbolize phenology. Summer stratification is generally when surface waters were above 20°C, while spring and fall mixing occurred below this water temperature.

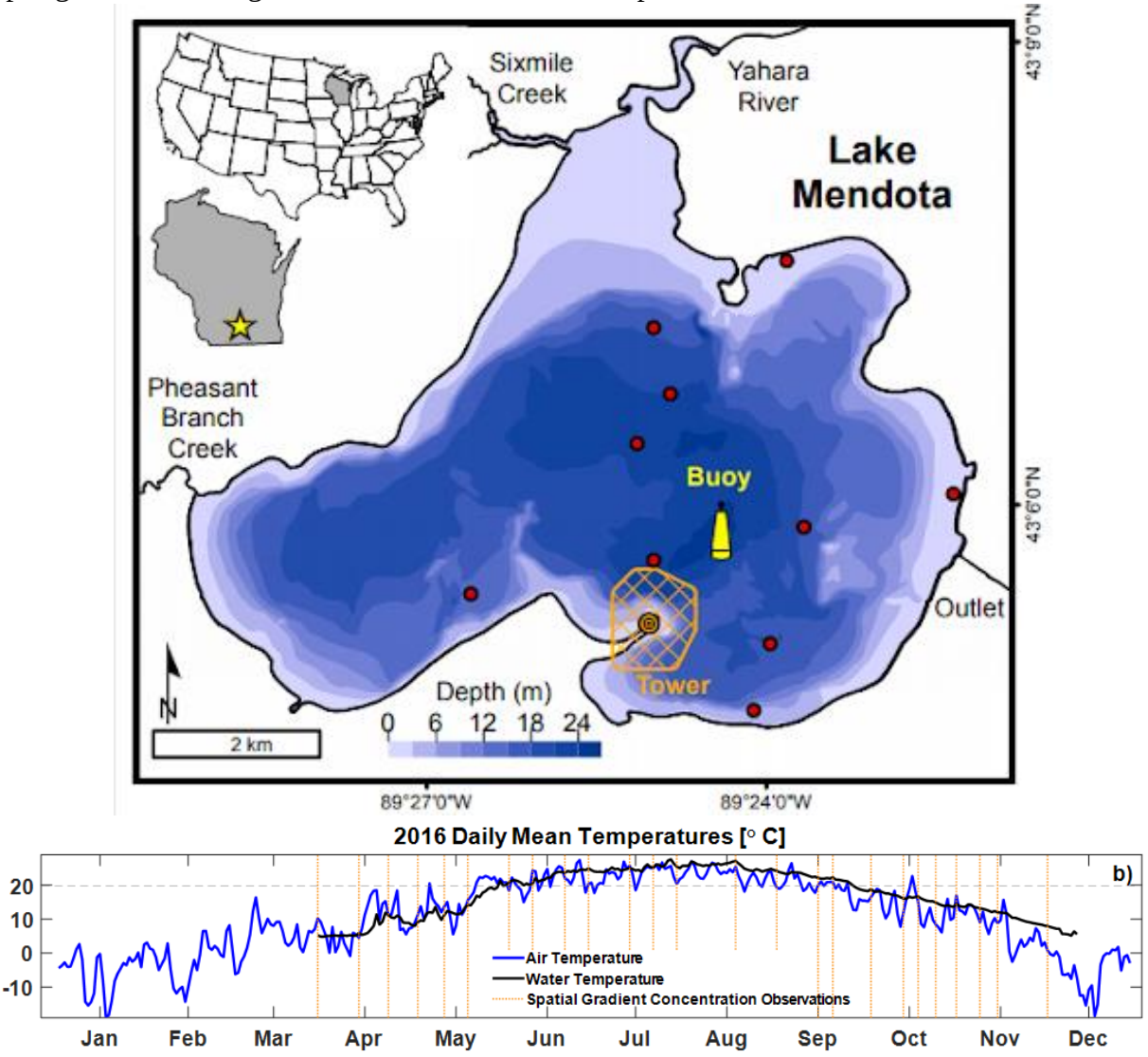

Figure 2

Panel (a) Map of picnic point EC tower and contributing footprint showing the distance of maximum flux and distance of 80% of the footprint. Average friction velocity (u*, panel b) and wind speed (panel c) measured from the eddy covariance tower, shown in 10° bins.

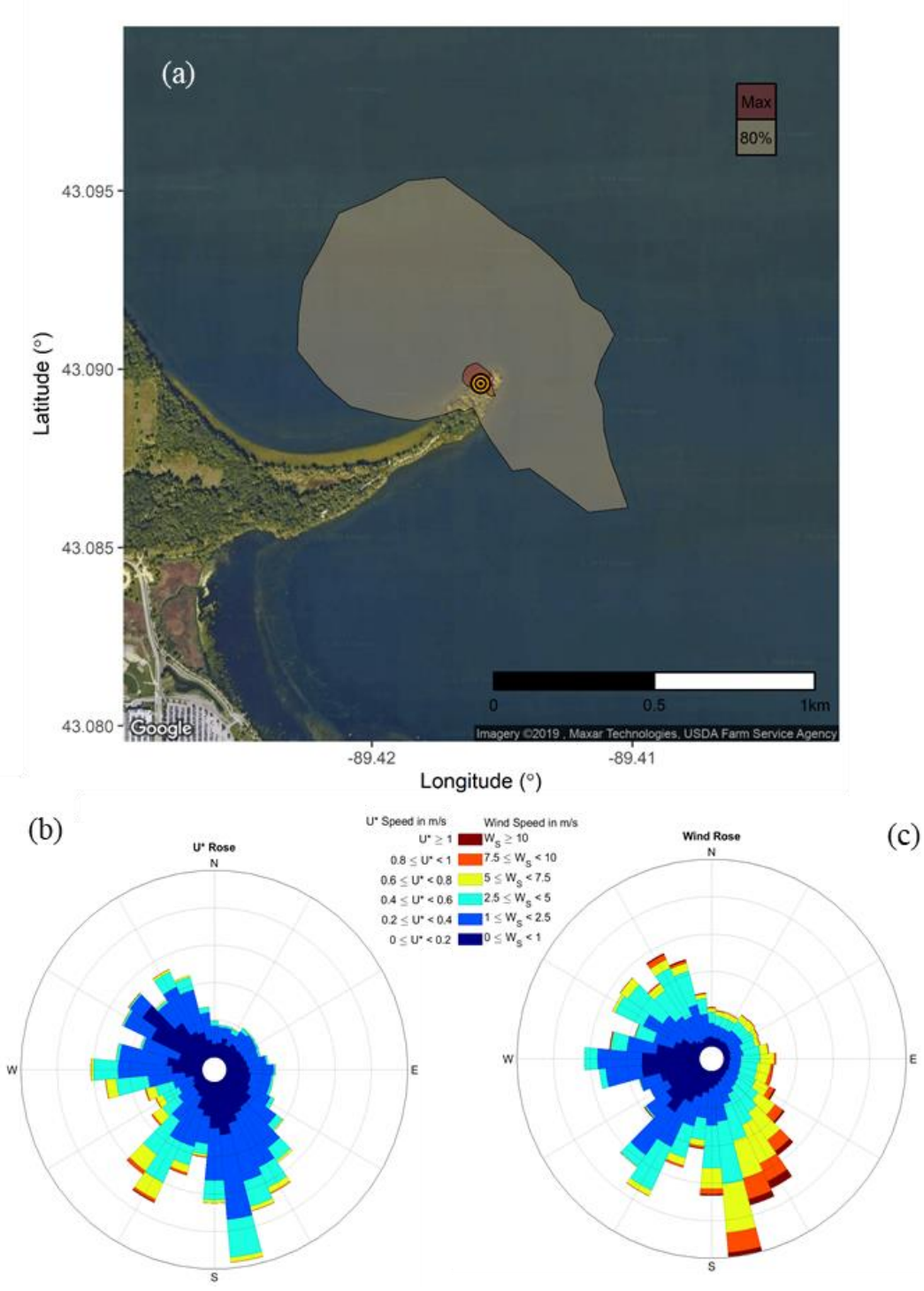

Figure 3

Panel A: Multi-year time series of mean daily CO_2 flux. F-pCO_2, fixed gradient concentration method, recorded from a stationary buoy (purple), S-pCO_2, spatial gradient concentration method, recorded by a moving boat (orange), and eddy covariance (green). Dates of flux chamber measurements shown as brown dotted vertical line. Panels B-D: Hourly three day subsets from spring, summer, and fall, centered on when FC data was collected. F-pCO_2 (purple), and EC (green) being 30-minute data, and FC (brown) are every 4 hours for a diel cycle.

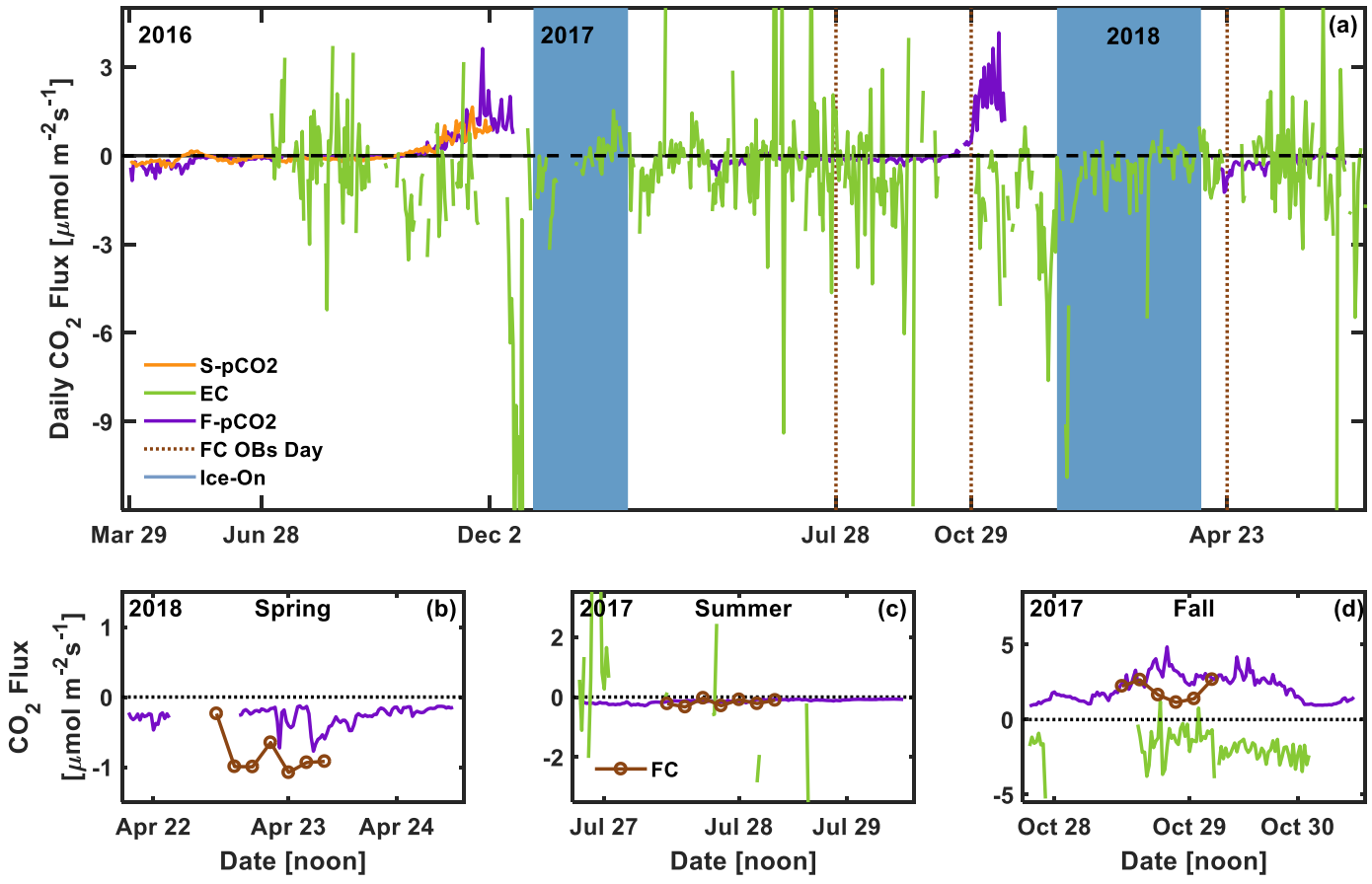

Figure 4

Histograms of seasonal daily CO_2 gas fluxes. Spatial S-pCO_2 fluxes (orange), fixed F-pCO_2 fluxes (purple), EC fluxes (green) for spring 2016 to spring 2018 and three seasons of FC mean fluxes in 2016 (brown).

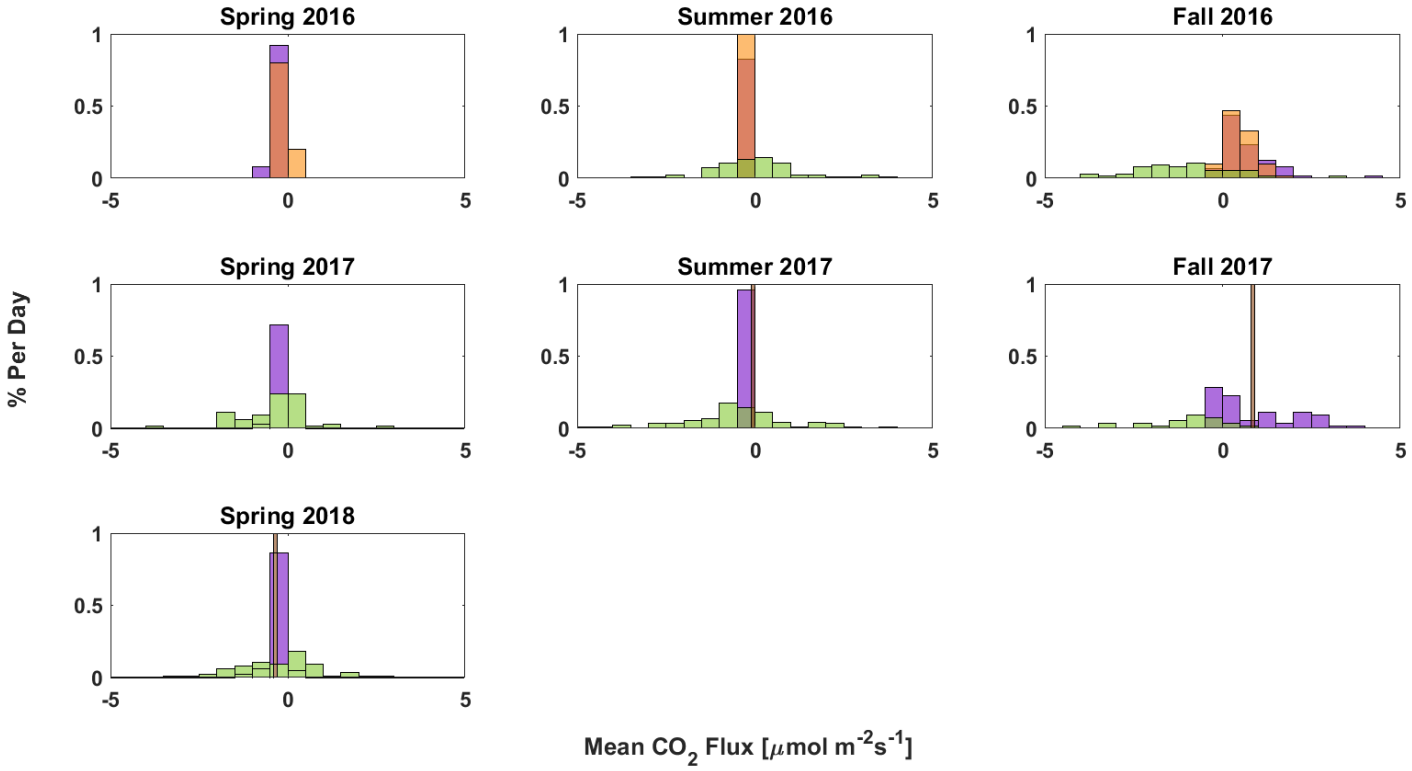

Figure 5

Cumulative summation of lake-atmosphere CO_2 fluxes. Flux estimates using the S-pCO_2 method (bold orange), from ten random points across the lake (orange), and within the tower footprint (orange dashed line), EC (green) and EC only during day (8AM-12PM, green dashed line), and the F-pCO_2, method (purple) and fixed boundary layer method during the day (8AM-12PM, purple dashed line).

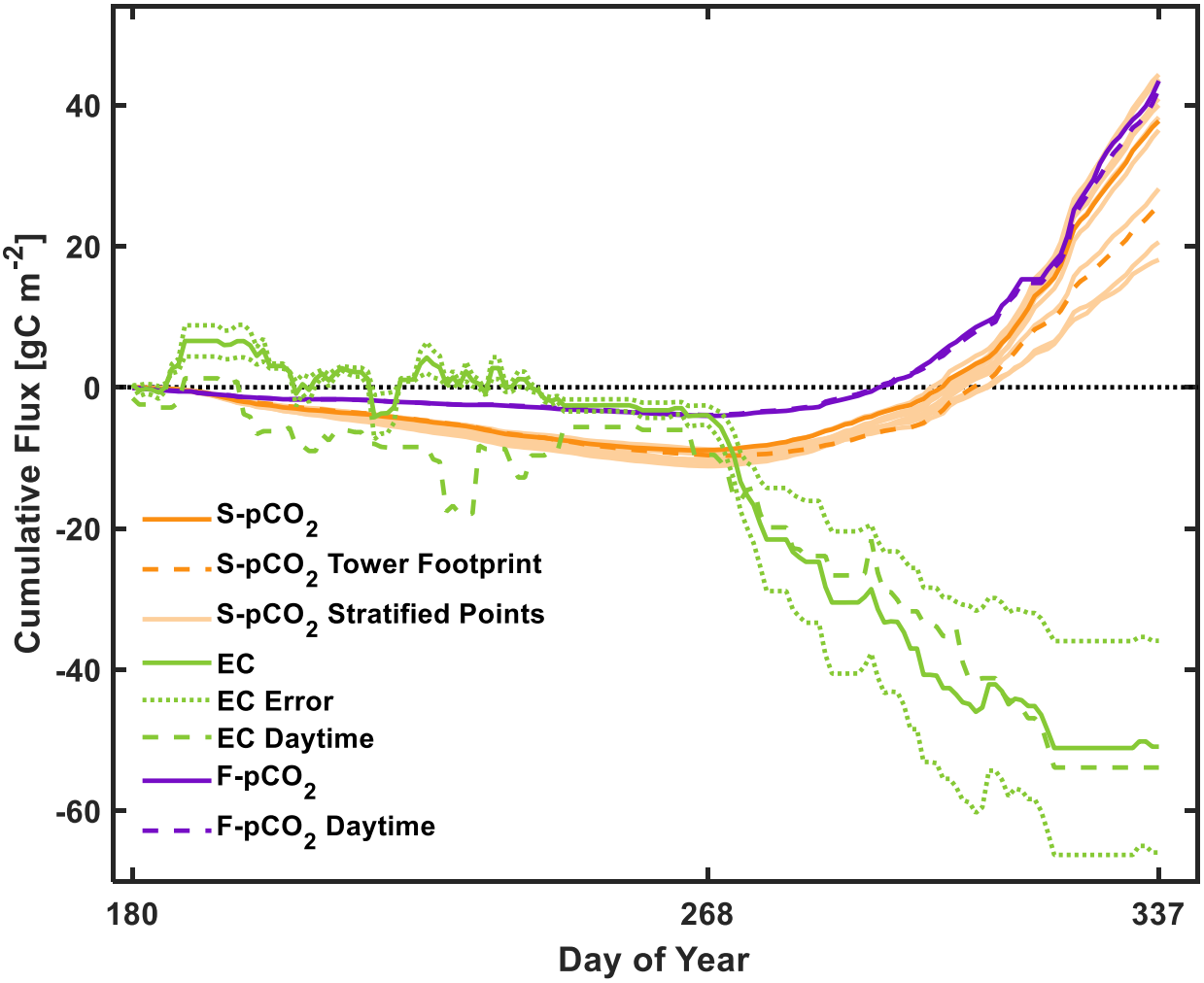

636 Figure 6 Daily mean S-*p*CO fluxes versus F-pCO_2 (panel a) and EC (panel b). Summer data are
637 plotted as open circles, fall data as *. Linear regression line (dashed) and one-to-one line
638 (dotted). Statistics (*p* and R^2) for linear regression included.
639

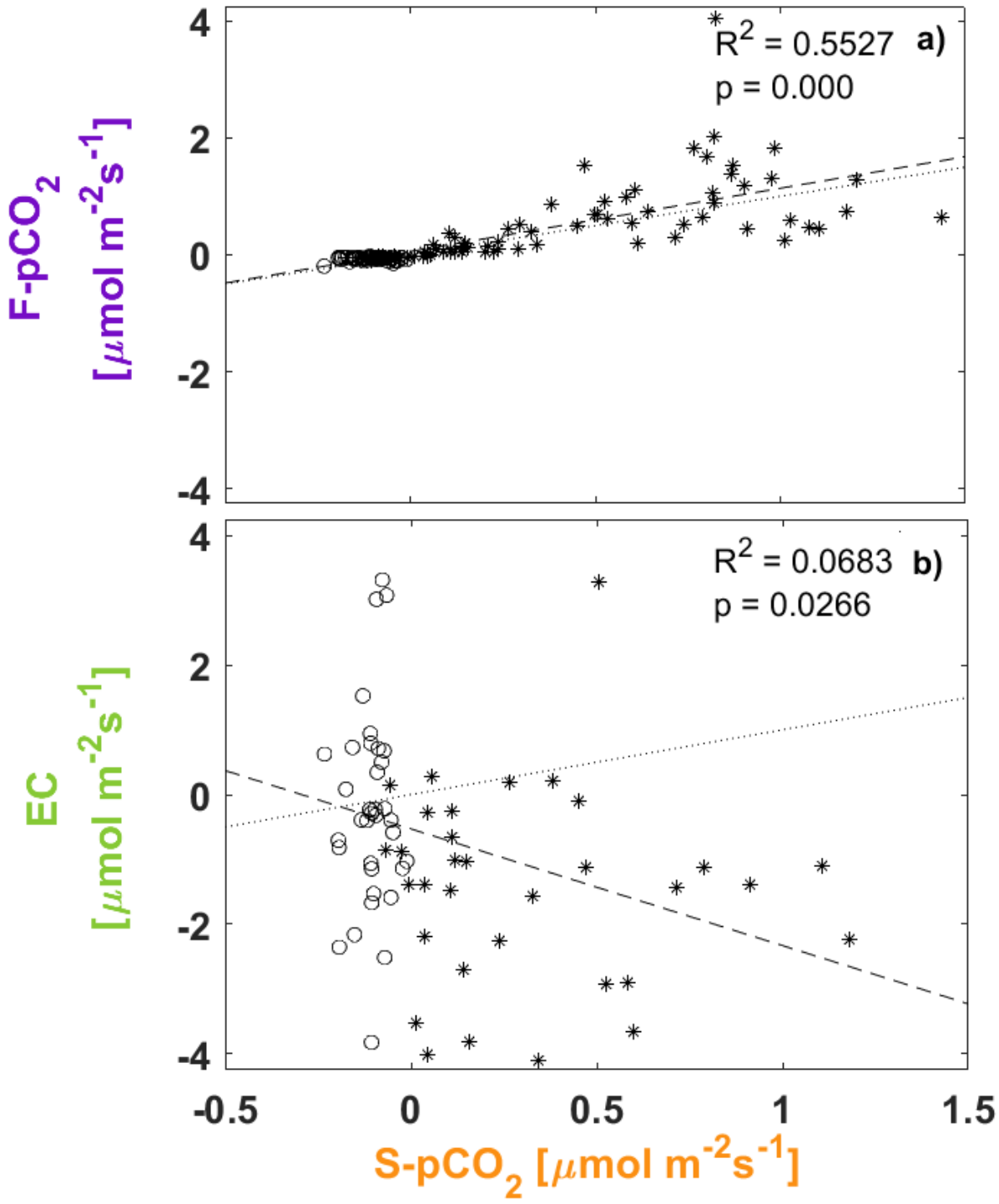

640

Figure 7 Fourier power spectral decomposition of daily EC (green), F-pCO_2 (purple) and S-pCO_2 (orange) CO_2 flux.